This is an *Accepted Manuscript*, which has been through the Royal Society of Chemistry peer review process and has been accepted for publication.

Accepted Manuscripts are published online shortly after acceptance, before technical editing, formatting and proof reading. Using this free service, authors can make their results available to the community, in citable form, before we publish the edited article. We will replace this *Accepted Manuscript* with the edited and formatted *Advance Article* as soon as it is available.

You can find more information about *Accepted Manuscripts* in the **Information for Authors**.

Please note that technical editing may introduce minor changes to the text and/or graphics, which may alter content. The journal's standard **Terms & Conditions** and the **Ethical guidelines** still apply. In no event shall the Royal Society of Chemistry be held responsible for any errors or omissions in this *Accepted Manuscript* or any consequences arising from the use of any information it contains.

WS$_2$ 2D Nanosheets in 3D Nanoflowers

Arunvinay Prabakaran, *[a] Frank Dillon,[a] Jodie Melbourne, [a] Lewys Jones, [a] Rebecca J Nicholls, [a] Phil Holdway, [a] Jude Britton, [a] Antal A Koos, [a] Peter D Nellist, [a] Alison Crossley, [a] Nicole Grobert [a]

In this work it has been established that 3D nanoflowers of WS$_2$ synthesized by chemical vapour deposition are composed of few layer WS$_2$ along the edges of the petals. An experimental study to understand the evolution of these
10 **nanostructures shows the nucleation and growth along with the compositional changes they undergo.**

The structural analogy of transition metal dichalcogenides[1] to graphite's layered structure, held together by van der Waals forces, prompted the synthesis and characterisation of inorganic
15 fullerene-like structures (IF)[2] and inorganic nanotubes (IN) of WS$_2$[3] in 1992[4] and MoS$_2$ in 1995.[5] The IF and IN structures resemble fullerenes and carbon nanotubes respectively[6]. They possess interesting mechanical[7] and electronic properties[8] which find applications in high temperature solid state lubricants and
20 catalysis.[9] Commercial quantities of these structures are synthesised from an oxide template which limit the morphology and enhance control[6]. However, since the discovery of graphene in 2004[10], two dimensional material systems have been in demand. Consequently the field is now actively pursuing
25 inorganic graphene analogues (IGA)[11], which due to their inherent band gap, are potential components in creating 2D heterostructures.[12] However, a reliable method to synthesize large quantities of these materials hasn't yet been established. Nanosheets of IGA possess excellent electronic[14] and optical
30 properties[15] which find applications in field effect transistors[16] and photodetectors[17] respectively. WS$_2$ nanomaterials in particular have shown potential applications as industrial catalysts in denitrogenation and hydrodesulphurization processes[18,19], high performance nanocomposites[20], and lithium
35 batteries.[21] Nevertheless, to exploit the properties of WS$_2$ nanomaterials, methods that enable precise control of the morphology are required.

In this work, a fast, catalyst free and easily scalable chemical vapour deposition (CVD) technique for the controlled synthesis
40 of well-defined tungsten disulphide (WS$_2$) nanomaterials on (100) silicon-based substrates using tungsten(VI)chloride (WCl$_6$- 2 mmol at 99.9 % purity) and sulphur (20 mmol at 80 % purity) as precursors is presented in Fig S1. The predominant morphology (>90 %) obtained by this process is WS$_2$ nanoflower
45 confirmed using electron microscopy as shown in Fig.1a and the chemistry verified using XRD and Raman in Fig S2. The morphology of the WS$_2$ nanostructures synthesised by the CVD
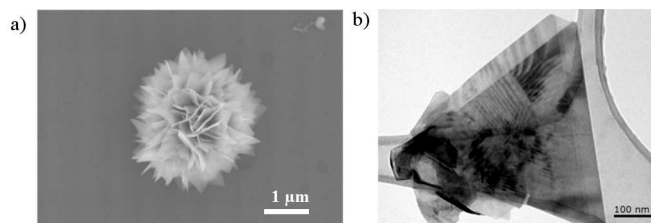

Figure 1.a) SEM image of 3D Nanoflower b) TEM images of a petal (flake)/2D nanosheet from a 3D nanoflower

50 technique can be tailored through the variation of just two key parameters: time and temperature. Though a similar strategy has been employed previously to obtain nanostructures of WS$_2$ and MoS$_2$[22], herein the process has been greatly simplified by using shorter time periods to enhance control and scalability. These
55 hierarchical nanostructures possess large surface area, easy accessibility to reaction sites and mechanical integrity which could are vital for application such as catalysis.[24]

WS$_2$ nanoflowers are composed of petals that resemble an equilateral triangular as shown in Fig 1b. Few layer edges have
60 been observed with atomic resolution using a double aberration corrected JEOL 2200 MCO operated at 200kV in Scanning Transmission Electron Microscopy (STEM) mode and a high angle annular dark field (HAADF) detector. Though nanoflowers were reported in 2004[22], as yet, a detailed analysis of their
65 structure has not been undertaken. This study looks to comprehend the structure of the nanoflower by disassembling it with the help of sonication. The nanoflowers disassembled into triangular petals (flakes) on sonication with one corner always broken, suggesting that these triangles are connected at only one
70 of the edges to form the assembly of 3D nanoflowers. We observed 10-100's of these triangular petals combining together to form spherical nanoflower structures as suggested by Li *et al.*[22] and evident from the Scanning Electron Microscope (SEM) micrograph in Fig 1a.

75 For WS$_2$, molecular sheets stacked together with spacing of 0.62 nm and an in-plane lattice spacing of 0.31 nm. In Fig 2a, a cluster of the petals which constitute a nanoflower is visualised from the edge view (beam perpendicular to c-axis), to reveal 6-8 molecular layers of WS$_2$. These WS$_2$ were stacked on top of each
80 other to form the petals. The distribution of the number of molecular layers to form the petal is not very uniform and varies from few layer (2-4) to increased number of layers up to 12/14. With the beam parallel to the c axis, the hexagonal packing can be clearly observed at the edges where the number of layers have
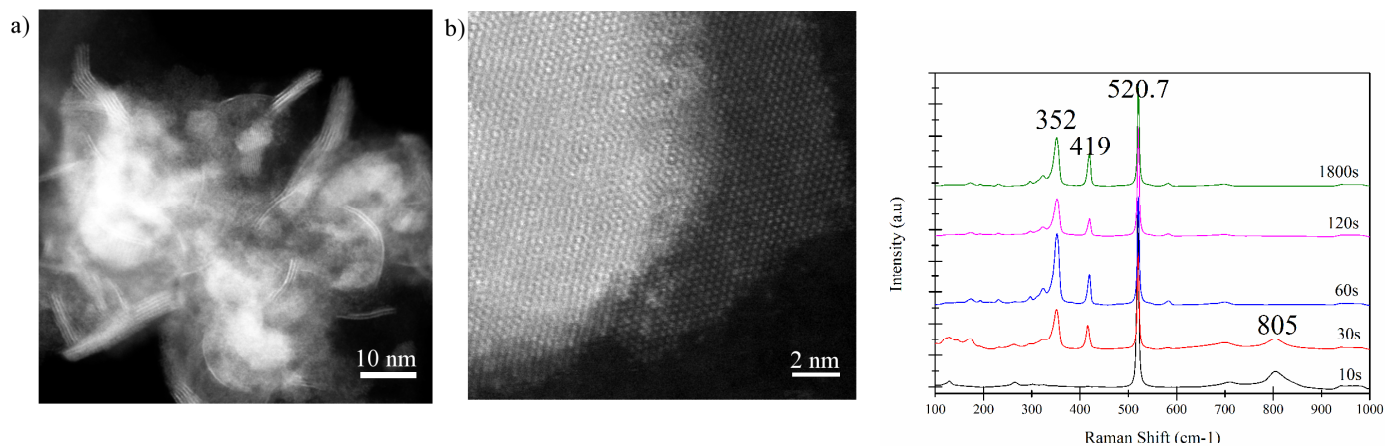85 reduced considerably to reveal mono- and bi-layer regions.

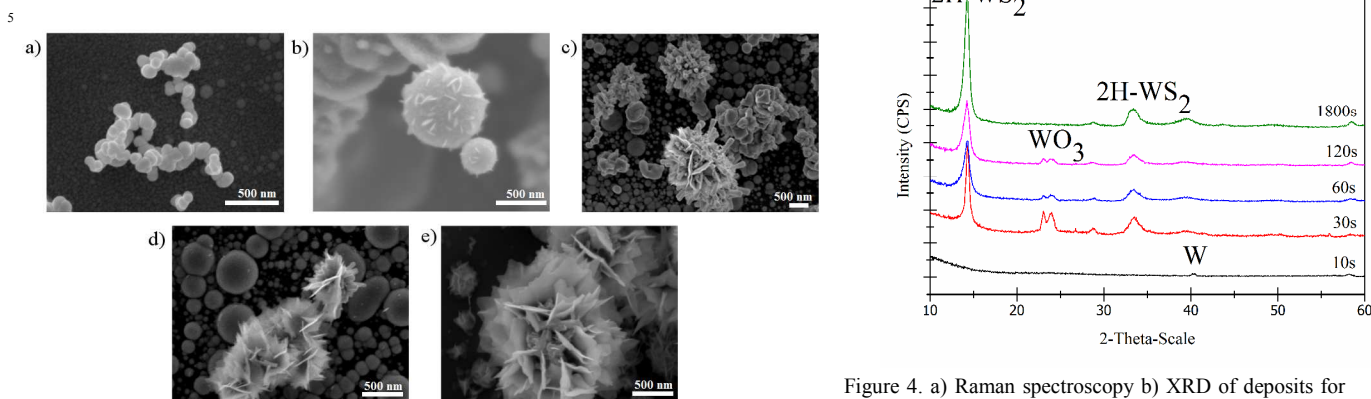Figure 2. STEM image depicting a) stacking of atomic layers in petal; b) atomic layers in WS$_2$ flake

Figure 3. Evolution of nanoflower structure with progress in time periods from 10s to 1800s at 850ºC

Figure 4. a) Raman spectroscopy b) XRD of deposits for various time periods from 10s to 1800s at 850ºC

This is a significant observation since it highlights that the nanoflowers are composed of few layer nanosheets at the edges. These few layer (mono- and bi-layer) edges are visible in the Fig 2b. As we move towards the centre of the petal the layers stack up progressively forming Moiré fringes which are visible near the centre of the petal.

In order to understand the evolution of these structures, short time nucleation experiments were carried out. The process parameters were similar to the CVD experiments employed to produce nanoflowers. However, the nucleation experiments were performed at very short time periods ranging from 10 s, 30 s, 60 s, and 120 s to 1800 s. The different stages of nucleation of the nanoflower are shown in Fig 3 and clearly shows the evolution process involved in forming these nanostructures. These different stages of evolution have also been studied using XRD and Raman spectroscopy and the results are shown in Fig. 4a and 4b respectively. Initially, nanoparticles of tungsten are formed, as confirmed by XRD at 10 s in Fig 4b. These particles are usually agglomerated as seen in Fig 3a. Oxidation of these nanoparticles over time was observed with the aid of EDX as presented in Fig S3. As reaction time was increased to 30 s, intermediate phases of tungsten- oxide and sulphide were observed as evident from the

WO$_3$ and WS$_2$ peaks in XRD. This could be sulphur progressively reacting with the oxide nanoparticles, as proposed by Tenne *et al.*[22], forming flake like structures on the surface, visible in Fig. 3b. The oxides may be formed when particles are oxidised when exposed to the atmosphere while transferring them for characterisation. The morphology after 60 s in Fig.3c shows the formation of petals from these particles and also the presence of tubular structures. With time, the tubular morphology disappears and only flakes are observed as in Fig 3d. Over longer time periods of 1800 s all of the tubular structures observed in Fig 3c & 3d are converted to flakes and flowers with predominantly large flakes/ petals as observed from Fig.3e and they exhibit characteristic WS$_2$ signals in Raman and XRD.

The synthesis process observed in this work seems to follow a combination of the mechanisms described previously in literature. W species are formed in the first 10 s, which are transformed into intermediate species of WO$_x$S$_y$ over 120 s, which eventually form a pure WS$_2$ phase after 300 s (5 min). This is determined by XRD, which clearly shows the suppression of oxide phases and dominance of sulfide phase with the increase in time from 10 s to 1800 s. Raman spectroscopy also shows the characteristic A$_1$g (352 cm^{-1}) and E$_2$g (420 cm^{-1}) belonging to

WS$_2$ phase which feature in the later stages of the process. Thus the initial phase of the experiment shows the presence of an oxide phase in both XRD and Raman. The source of this oxygen is uncertain and is difficult to trace.

Tenne *et al.*[23] highlight a similar mechanism for the formation of IF-WS$_2$ nanoparticles using WCl$_n$ and H$_2$S precursors. A major difference from that work is the formation of WS$_2$ nanosheets on the surface of the nanoparticle in random directions leading to nanoflower formation in contrast to confined growth in IF-WS$_2$. It is reported that the WCl$_n$ on heating first forms W species, possibly WCl$_x$S$_y$, which on subsequent reaction leads to the formation of a pure WS$_2$ phase. Another mechanism proposed based on TEM-EDS, was amorphous WS$_3$ formation enhancing IF-WS2 formation through sulphur abstraction and crystallization[22]. Li *et al.*[22] reported the use of sulphur both as a reductant and sulphurisation agent at the same time. They reported a self-redox and metathesis reaction, resulting in a stepwise sulphurisation of MoCl$_5$ to form MoS$_x$Cl$_y$ intermediate at low temperatures of 515 ^{o}C and pure MoS$_2$ phase at 800 ^{o}C. This same mechanism is likely to hold for WS$_2$.

The potential use of nanoflowers as a precursor/source for nanosheets would make it an attractive process for 2D material as large amounts (grams) of these nanoflowers can be produced by a relatively simple CVD process. Furthermore, these nanoflowers could be studied for applications such as catalysts for hydrogen evolution due to the presence of few layer edges.

Conclusions

In summary, we have reported the presence of 2D nanosheets in 3D nanoflowers of WS$_2$ nanomaterials. Using aberration corrected scanning transmission electron microscopy, we observed the presence of few layer WS$_2$ at the edges of these 2D nanosheets/petals and also the progressive stacking of these layers to form the petals that in turn give the 3D nanoflower morphology. This study eludes to the possibility of using 3D nanoflowers, which are relatively easy to synthesize using a simple scalable atmospheric chemical vapour deposition method, as precursors for 2D nanosheets. In addition, the process of nucleation has been followed closely to reveal the role of oxide nanoparticles in the formation of these nanostructures.

Notes and references

[a] *Department of Materials, University of Oxford, Parks Road, OX1 3PH, UK. E-mail:* nicole.grobert@materials.ox.ac.uk

1. J. A Wilson and A D. Yoffe, *Adv. Phys.*, 1969, **18**, 193–335.

2. Y. Feldman, G. L. Frey, M. Homyonfer, V. Lyakhovitskaya, L. Margulis, H. Cohen, G. Hodes, J. L. Hutchison, and R. Tenne, *J. Am. Chem. Soc* 1996, **2**, 5362–5367.

3. A. Rothschild, J. Sloan, and R. Tenne, *J. Am. Chem. Soc* 2000, 5169–5179.

4. G. Tenne, R. Margulis, L. Genut, M. & Hodes, *Nature*, 1992, **360**, 444–446.

5. Y. Feldman, E. Wasserman, D. J. Srolovitz, and R. Tenne, *Science*, 1995, **267**, 222–5.

6. R. Tenne, *Nat. Nanotechnol.*, 2006, **1**, 103–111.

7. Y. Q. Zhu, T. Sekine, Y. H. Li, M. W. Fay, Y. M. Zhao, C. H. Patrick Poa, W. X. Wang, M. J. Roe, P. D. Brown, N. Fleischer, and R. Tenne, *J. Am. Chem. Soc.*, 2005, **127**, 16263–72.

8. G. Seifert, H. Terrones, M. Terrones, G. Jungnickel, and T. Frauenheim, *Phys. Rev. Lett.*, 2000, **85**, 146–9.

9. R. R. Chianelli, M. H. Siadati, M. P. De la Rosa, G. Berhault, J. P. Wilcoxon, R. Bearden, and B. L. Abrams, *Catal. Rev.*, 2006, **48**, 1–41.

10. K. S. Novoselov, a K. Geim, S. V Morozov, D. Jiang, Y. Zhang, S. V Dubonos, I. V Grigorieva, and a a Firsov, *Science*, 2004, **306**, 666–9.

11. S. Z. Butler, S. M. Hollen, L. Cao, Y. Cui, J. A. Gupta, H. R. Gutie, T. F. Heinz, S. S. Hong, J. Huang, A. F. Ismach, E. Johnston-halperin, M. Kuno, V. V Plashnitsa, R. D. Robinson, R. S. Ruoff, S. Salahuddin, J. Shan, L. Shi, O. M. G. Spencer, M. Terrones, W. Windl, and J. E. Goldberger, *ACS Nano,* 2013.

12. A. K. Geim and I. V Grigorieva, *Nature*, 2013, **499**, 419–25.

13. H.Terrones, F. Lopez-Urias and M.Terrnoes, *Nature Scientific reports*, 2013, **3**, 1549

14. Z. Zeng, Z. Yin, X. Huang, H. Li, Q. He, G. Lu, F. Boey, and H. Zhang, *Angew. Chem. Int. Ed. Engl.*, 2011, **50**, 11093–7.

15. A. Splendiani, L. Sun, Y. Zhang, T. Li, J. Kim, C.-Y. Chim, G. Galli, and F. Wang, *Nano Lett.*, 2010, **10**, 1271–5.

16. B. Radisavljevic, a Radenovic, J. Brivio, V. Giacometti, and a Kis, *Nat. Nanotechnol.*, 2011, **6**, 147–50.

17. N. Huo, S.Yang, Z.Wei, Shu-Shen Li, J.B. Xia and J. Li, *Nature Scientific Reports*, 2014, doi:10.1038/srep05209

18. A. Sobczynski, A. Yildiz, A. J. Bard, A. Campion, M. A. Fox, T. Mallouk, S. E. Webber, and J. M. White, *J. Phys. Chem* 1988, 2311–2315.

19. P. Luque, E. Medina, and A. Olivas, *Jour. of Matl Sci Eng B* 2012, **2**, 569–574.

20. L. Rapoport, N. Fleischer, and R. Tenne, *J. Mater. Chem.*, 2005, **15**, 1782.

21. G. X. Wang, S. Bewlay, J. Yao, H. K. Liu, and S. X. Dou, *Electrochem. Solid-State Lett.*, 2004, **7**, A321.

22. X.-L. Li, J.-P. Ge, and Y.-D. Li, *Chemistry*, 2004, **10**, 6163–71.

23. A. Margolin, F. L. Deepak, R. Popovitz-Biro, M. Bar-Sadan, Y. Feldman, and R. Tenne, *Nanotechnology*, 2008, **19**, 095601.

24. B.G. Choi, Y.S. Huh, W.H. Hong, H.J. Kim and H.K. Park, *Nanoscale*, 2012, 4, 5394.